CHINESE OPTICS LETTERS

Vol. 19, No. 3 | March 2021

Stable and high performance all-inorganic perovskite light-emitting diodes with anti-solvent treatment

Sajid Hussain[1,†], Ahmad Raza[1,†], Fawad Saeed[1], Abida Perveen[1], Yan Sikhai[1], Nasrud Din[1], Elias E. Elemike[2], Qianqian Huang (黄倩倩)[1], Alagesan Subramanian[1,*], Qasim Khan[1,3,**], and Wei Lei (雷 威)[1,***]

[1] Joint International Laboratory of Information Display and Visualization, School of Electronic Science and Engineering, Southeast University, Nanjing 210096, China

[2] Chemistry Department, North West University, Mafikeng, South Africa

[3] Institute of Microscale Optoelectronics, Shenzhen University, Shenzhen 518000, China

*Corresponding author: alaphy007@hotmail.com

**Corresponding author: qasim@szu.edu.cn

***Corresponding author: lw@seu.edu.cn

Received December 8, 2020 | Accepted January 19, 2021 | Posted Online March 9, 2021

Optoelectronic applications based on the perovskites always face challenges due to the inherent chemical composition volatility of perovskite precursors. The efficiency of perovskite-based light-emitting diodes (Pe-LEDs) can be enhanced by improving the perovskite film via solvent engineering. A dual solvent post-treatment strategy was applied to the perovskite film, which provides a synchronous effect of passivating surface imperfections and reduces exciton quenching, as evidenced by improved surface morphology and photoluminance. Thus, the optimized Pe-LEDs reach 17,866 cd · m^{-2} maximum brightness, 45.8 cd · A^{-1} current efficiency, 8.3% external quantum efficiency, and relatively low turn-on voltage of 2.0 V. Herein, we present a simple technique for the fabrication of stable and efficient Pe-LEDs.

Keywords: $CsPbBr_3$; light-emitting diode; solvent treatment; charge-carrier injection; perovskite LED.
DOI: 10.3788/COL202119.030005

1. Introduction

Organic and inorganic halide perovskites have attracted a lot of attention due to their extensive use in various applications and optoelectronic properties like broad band wavelength absorption, high photoluminance (PL), narrow full width at half-maximum (FWHM), band gap tunability, intrinsic photophysical stability[1], and their revolutionary optoelectronic application in perovskite-based light-emitting diodes (Pe-LEDs)[2–6]. Perovskite material is widely applied in light-emitting diodes (LEDs), lasers, and photodetectors[7]. Particularly, Pe-LED has been studied, and its efficiency has been significantly improved by enhancing the crystallinity and morphology of perovskite film as well as optimizing device structures[8,9]. Despite the advantages of the fast free exciton emission attenuation described above, it may help transfer non-radiant energy to trapped states, but the severe challenges of Pe-LEDs remain. Due to the short PL decay life, it indicates a serious non-radiant energy transfer to the trapped state. Among all perovskites, all-inorganic perovskites have attracted extraordinary attention due to their high heat resistance compared to organic perovskites[10,11].

For example, cesium lead bromide ($CsPbBr_3$) polycrystalline film-based Pe-LEDs offer an auspicious substitute technique to increase the device performance due to their higher thermal stability compared with organic-based perovskite methylammonium lead bromide ($MAPbBr_3$)-based Pe-LEDs. However, sensitivities to humidity, light, and heat are still the main challenges facing Pe-LEDs[12,13]. Nonetheless, various polycrystalline $CsPbBr_3$-based Pe-LEDs suffer from low brightness (L) and inefficiency due to their low film surface coverage and PL-quantum yield (PLQY)[4,6,13]. Engineering a completely covered $CsPbBr_3$ polycrystalline film with high PLQYs has been verified to be a significant prerequisite to improve both efficiency and luminance of Pe-LEDs. Post-treatments of organic compounds such as methyl acetate (MA), chlorobenzene (CB), ethanol (EtOH), and isopropanol (IPA) play an important role in achieving uniform thin films and preventing leakage currents, mostly during the single step spin-coating process[3,9,14,15].

However, energy level matching and unbalanced charge carrier injection are also serious issues hindering the high efficiency of perovskite-based optoelectronic devices[16]. A metal oxide, zinc oxide (ZnO)[17], as an electron transport layer (ETL) takes

a few edges like high electron mobility, better electron injection, and a good hole-blocking layer as compared to 1,3,5-tris(1-phenyl-1H-benzimidazol-2-yl) benzene (TPBi), TiO_2, and [6,6]-phenyl C_{61} butyric acid methyl ester (PCBM)[18–20]. On the other hand, coupled molecules such as poly(9-vinylcabazole) (PVK) exhibit a minimum energy barrier for hole injection at the emissive layer (EML) interface and thus are widely used as hole transport layer (HTL). However, hole mobility of PVK ($2.5 \times 10^{-6}\,cm^2 \cdot V^{-1} \cdot s^{-1}$) is 1000 times lower in magnitude than the electron mobility of ZnO ($1 \times 10^{-3}\,cm^2 \cdot V^{-1} \cdot s^{-1}$). The unequal mobilities of these layers then result in unbalanced charge injection into the EML and show poor device performance[21]. Replacing them with high hole mobility organic molecules such as poly[bis(4-phenyl(4-butylphenyl)amine] (poly-TPD) ($1 \times 10^{-4}\,cm^2 \cdot V^{-1} \cdot s^{-1}$) is a better choice for efficient hole injection in order to increase the efficiency of perovskite-based inverted LED devices[22].

Through a simple spin-coating technique, we have successfully designed and manufactured inverted perovskite LEDs with higher performance and stability. To improve the surface morphology, PL, and interfacial interaction between the transporting layers and active layer, a simple post-treatment strategy of applying MA while spinning, is followed by another solvent known as the anti-solvent, i.e., CB. As a result, the devices showed a low turn-on voltage (V_T) of 2.0 V and maximum luminance of 17,866 $cd \cdot m^{-2}$ at current efficiency of 45.8 $cd \cdot A^{-1}$. This initiative suggests a simple way to adjust rate of the carriers' injection along with reducing surface defects in optoelectronic devices and lighting technologies based on perovskites for their high resolution displays and cost-effective technology.

2. Experimental Section

The patterned fluorine-doped tin oxide (FTO) substrates were cleaned with detergent, deionized (DI) water, acetone, EtOH, and IPA for 15 min each using the ultrasonication cleaner and treated with UV ozone for 30 min before use. The ETL ZnO nanoparticles (NPs) (25 $mg \cdot mL^{-1}$ in butanol, filtered through a 0.22 μm N66 filter) were spin-coated on the substrate at 2000 r/min for 40 s and annealed at 140°C for 10 min. The active layer perovskite precursor solution CsBr and $PbBr_2$ with a molar ratio of 1.2:1 (0.3 mol/L) was mixed in anhydrous dimethyl sulfoxide (DMSO) (80°C, 4 h, 800 r/min), spun onto the ZnO NPs at 2000 r/min for 50 s along with the dropped MA delay of 5 s after starting the spin coater, and finally treated with an anti-solvent CB perovskite layer with same speed. Afterward, poly-TPD (10 $mg \cdot mL^{-1}$ in chloroform) as an HTL was spin-coated onto the perovskite film at 2500 r/min for 40 s. Finally, Au was deposited by thermal deposition through a shadow mask. The active area of our fabricated devices was 0.04 cm^2. All of the fabrication was done in ambient conditions.

3. Result and Discussion

Fabrication of the uniform, continuous, and pinhole-free $CsPbBr_3$ film remains a challenge. Scanning-electron microscopy (SEM) images of perovskite film in Fig. 1(a) reveal that the as prepared $CsPbBr_3$ film is discontinuous on ZnO NPs. The coverage of the polycrystalline $CsPbBr_3$ is too poor because of the high crystallization rate of the perovskites. By observation through SEM images, it is roughly estimated that the entire coverage of perovskite film without any solvent treatment was very low, which is reliable with a previously reported treatment onto ZnO NPs[23]. Incomplete surface coverage of the perovskite film caused leakage current limiting to the Pe-LED output. Furthermore, for increases in the morphology of perovskite film treated with only CB solvent, there is a small increase in the surface distribution. Conversely, by dropping MA on the $CsPbBr_3$ precursor surface after 5 s delay as spin-coating begins, well-covered $CsPbBr_3$ polycrystalline films were obtained on the ZnO NPs layer, as shown in Fig. 1(b). The $CsPbBr_3$ films with homogeneous crystals showed a higher surface coverage of the film. Such a crystalline film enhances the PL, reduces the leakage current, and increases the device performance. However, there are still many pinholes scattered around the film; we further treated the film with an anti-solvent (CB) and dropped it onto $CsPbBr_3$ film already treated with MA for 30 s, which increased the crystal size of the perocfvskite, as shown in Fig. 1(c).

In order to investigate the crystal structure, an X-ray diffraction (XRD) measurement of perovskite film deposited on the FTO was performed. The XRD patterns of $CsPbBr_3$ film prepared with and without solvent treatment are shown in Fig. 2(a). All of the samples show similar perovskite properties, and all crystallographic features are in good agreement with the orthorhombic tetragonal $CsPbBr_3$ phase.

However, good crystallographic properties are exhibited when dropping anti-solvent CB onto the MA-treated perovskite film, which is also evidence of improved device performance.

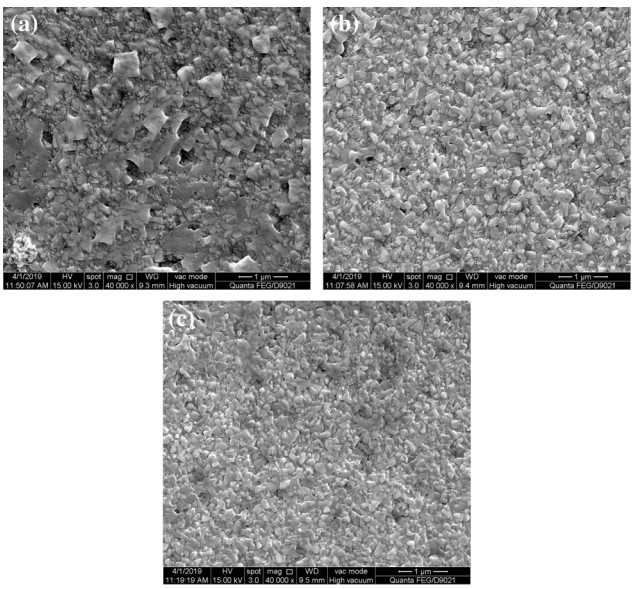

Fig. 1. Scanning electron microscopy (SEM) images of perovskite films (a) without MA, (b) with dropped MA after delay of 5 s, and (c) treated with anti-solvent CB and MA.

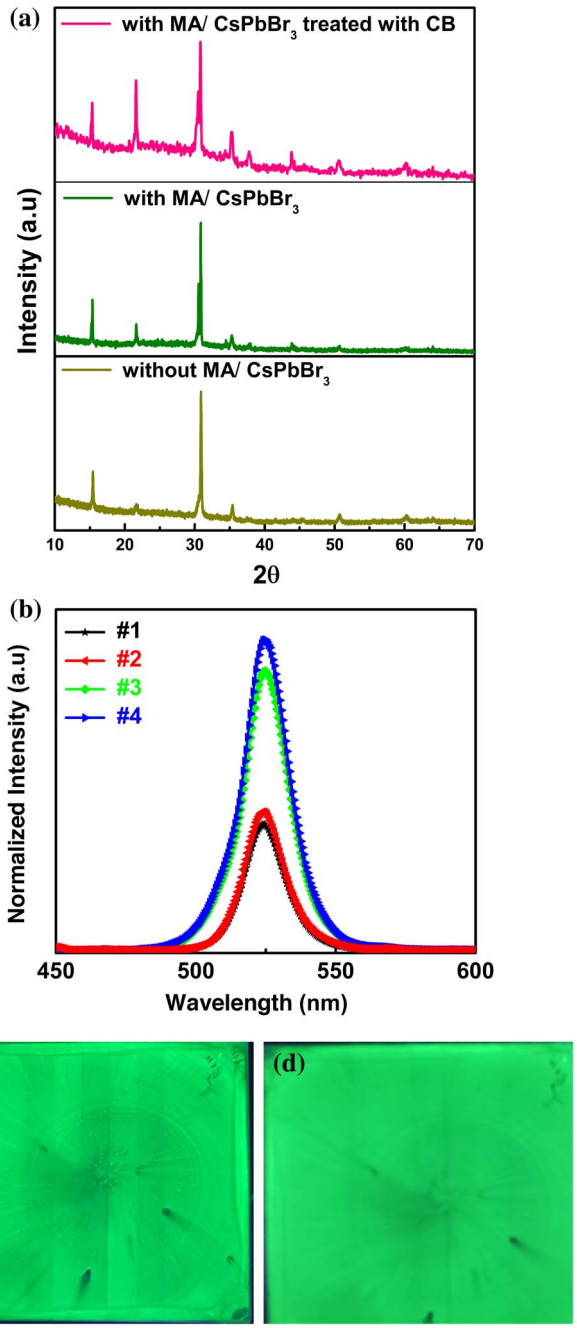

Fig. 2. (a) X-ray diffraction (XRD) patterns without MA/$CsPbBr_3$, with MA/$CsPbBr_3$, and with MA/$CsPbBr_3$ treated with anti-solvent CB. (b) Normalized PL, (c) PL image only with MA-treated perovskite film, and (d) PL image of perovskite film treated with CB and MA.

High performance of Pe-LEDs can be understood by the effective improvement in the fluorescence quantum efficiency, which can be improved by solvent treatment of the perovskite film. A good comparison between the PL emission of $CsPbBr_3$ films with/without solvent behavior is shown in Fig. 2(b). An instant transition has been noted at around 524.5 nm in the PL emission band with narrow FWHM of 17 nm for all of the perovskite films, with a difference of enhanced PL emission with solvent-treated films, whereas, PLQYs with anti-solvent-treated $CsPbBr_3$ perovskite film are ~20.1%, which is higher than those without solvent-treated $CsPbBr_3$ films of ~15.3%. Figure 2(c) shows PL images under the UV light at 365 nm, which signifies that with solvent treatment we can obtain a film with small and closely packed grains, which enhances the surface coverage and quality of perovskite film, ultimately enhancing the performance of the device.

The inverted Pe-LEDs with either pristine or post-treated $CsPbBr_3$ (EML) were fabricated, as shown in Figs. 3(a) and 3(b) with the following structure: FTO/ZnO/$CsPbBr_3$/Poly-TPD/Au. An anti-solvent CB was dropped onto the MA-treated perovskite film in order to increase the morphology and surface coverage; this device is denoted as "#4". For comparison, we tested with same structure without dropping the anti-solvent CB onto the solvent-treated MA perovskite film and the device is denoted as "#3"; whereas, we understand the mechanism of the perovskite film as a reference device with only solvent-treated CB, denoted as "#2". Any device without any solvent treatment is denoted as "#1". Here FTO, ZnO, poly-TPD, and Au are used as the cathode, ETLs, HTLs, and anode, respectively.

The performance of $CsPbBr_3$-based devices is visualized and summarized in Fig. 4 and Table 1. Figures 4(a)–4(d) represent

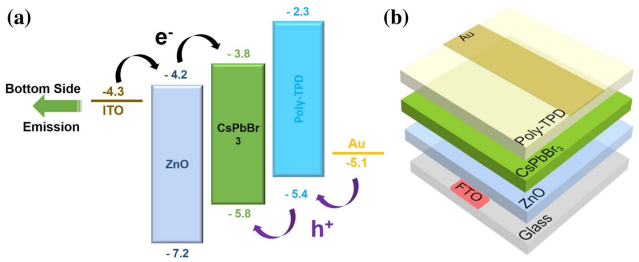

Fig. 3. (a) Energy level diagram of the Pe-LEDs. (b) Schematic of device structure.

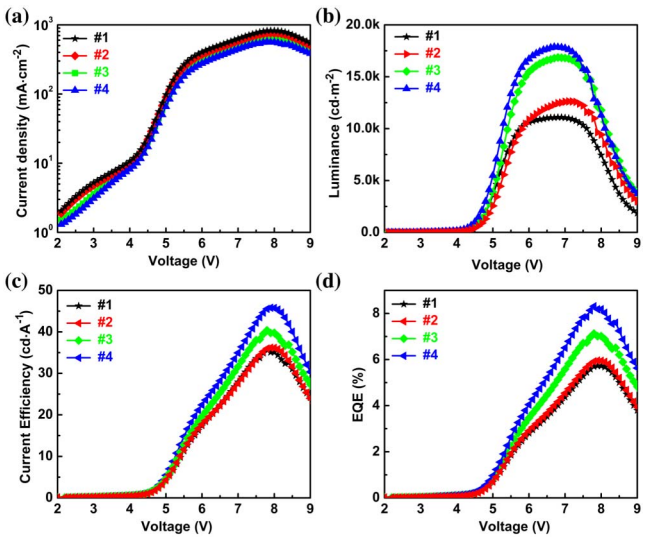

Fig. 4. Comparison results: (a) *J-V*, (b) luminance-*V*, (c) CE-*V*, and (d) EQE-*V*.

Table 1. Characteristics of the Measured Pe-LED Devices.

Device No.	Structure	V_T(V)	L_{max} (cd·m^{-2})	CE_{max} (cd·A^{-1})	EQE_{max} (%)
1	FTO/ZnO/$CsPbBr_3$ (with/without MA)/poly-TPD/Au	2.4	11,088	35.6	5.7
2	FTO/ZnO/$CsPbBr_3$ (with CB)/poly-TPD/Au	2.4	12,622	36.1	5.9
3	FTO/ZnO/$CsPbBr_3$ (with MA)/poly-TPD/Au	2.1	16,855	40.4	7.1
4	FTO/ZnO/$CsPbBr_3$ (with MA)-dropped CB/poly-TPD/Au	2.0	17,866	45.8	8.3

the summarized characteristics of the devices with and without anti-solvent treatment. Figure 4(a) shows the current density–voltage (*J-V*) characteristics of all of the fabricated devices. The lowest current density (*J*) of device #4 is an indication of the crystalline perovskite film blocking the short-circuit current paths in the device, as revealed in the SEM images. The better surface coverage of the perovskite film in turn results in higher device performance due to better charge injection in the EML. The compared luminance performances of the Pe-LEDs are shown in Fig. 4(b). The improvement in luminance of device #4 with anti-solvent-treated perovskite film, as compared to that of devices #1, 2, and 3, indicates that the minimized short circuit as well as an incredible enhancement in CE is found, as shown in Fig. 4(c), and the higher external quantum efficiency (EQE) for device #4 [Fig. 4(d)] is dedicated to the improved surface morphology and affects the performance of the device due to solvent treatment.

The stability of all of the devices was measured in ambient conditions at 50% humidity without any encapsulation. Figure 5(a) describes the details of the stability results, where device #4 shows excellent stability when compared to the rest of the devices. The surplus of electrons due to greater mobility of ZnO as compared to the low hole mobility of poly-TPD induces high electron conductivity, resulting in increased exciton quenching and reduced radioactive recombination in the active region. Besides, the charge unbalance into the EML is also one of the major causes to make the LED device unstable and with low efficiency. To check the carrier's injection mechanism into the EML, we studied the hole-only device (HOD) and electron-only device (EOD), showing the well-balanced charge injection and the improved device performance, as shown in Fig. 5(b).

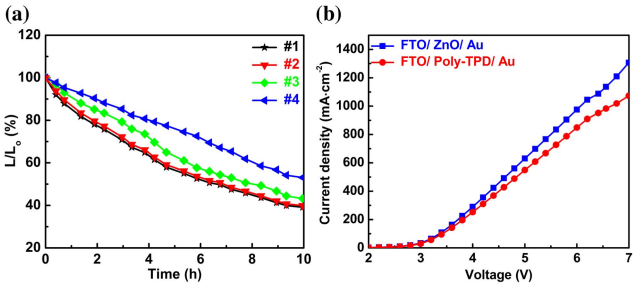

Fig. 5. (a) Stability characteristics of different devices and (b) comparison between the HODs and EODs.

4. Conclusion

We have presented a simple and facile method for obtaining high quality $CsPbBr_3$ perovskite film for efficient Pe-LEDs. Dropping anti-solvent CB onto MA treated $CsPbBr_3$ film can gain high coverage of the active layer with nanocrystal growth in ambient conditions. The fast crystallization rate has a diverse effect on device performance and its stability. Pe-LEDs treated with solvent exhibit luminance of 17,866 cd · m^{-2} and current efficiency of 45.8 cd · A^{-1}, which is one of the highest efficiencies of all Pe-LEDs solution-based inorganic $CsPbBr_3$, and also show strong stability. Most significantly, the film treated with solvent is efficient and more durable against environmental moisture and oxygen, which is a promising material for the fabrication of all-inorganic $CsPbBr_3$-based LEDs with high efficiency.

Acknowledgement

This work was financially supported by the National Key Research and Development Program of China (Nos. 2018YFE0125500 and 2016YFB0401600), Program 111_2.0 in China (BP0719013), National Natural Science Foundation of China (Nos. 61775034, 51879042, 61674029, and 12005038), Research Fund for International Young Scientists (No. 62050410350), International Cooperative Research Project of Jiangsu Province (No. BZ2018056), Leading Technology of Jiangsu Basic Research Plan (No. BK20192003), Aeronautical Science Foundation of China (No. 201951069001), and Jiangsu Province College Graduate Research Innovation Program (No. KYLX16_0213).

†These authors contributed equally to this work.

References

1. K. Qasim, B. Wang, Y. Zhang, P. Li, Y. Wang, S. Li, S. T. Lee, L. S. Liao, W. Lei, and Q. Bao, "Solution-processed extremely efficient multicolor perovskite light-emitting diodes utilizing doped electron transport layer," Adv. Funct. Mater. **27**, 1606874 (2017).
2. Y. C. Kim, S. D. Baek, and J. M. Myoung, "Enhanced brightness of methylammonium lead tribromide perovskite microcrystal-based green light-emitting diodes by adding hydrophilic polyvinylpyrrolione with oleic-modified ZnO quantum dot electron transporting layer," Alloys Compd. **786**, 11 (2019).

3. Z. Wang, Z. Luo, C. Zhao, Q. Guo, Y. Wang, F. Wang, X. Bian, A. Alsaedi, T. Hayat, and Z. Tan, "Efficient and stable pure green all-inorganic perovskite $CsPbBr_3$ light emitting diodes with a solution-processed NiO_x interlayer," J. Phys. Chem. C **121**, 28132 (2017).
4. W. Li, Y. X. Xu, D. Wang, F. Chen, and Z. K. Chen, "Inorganic perovskite light emitting diodes with ZnO as the electron transport layer by direct atomic layer deposition," Org. Electron. **57**, 60 (2018).
5. J. Li, X. Shan, S. G. R. Bade, T. Geske, Q. Jiang, X. Yang, and Z. Yu, "Single-layer halide perovskite light-emitting diodes with sub-band gap turn-on voltage and high brightness," J. Phys. Chem. Lett. **7**, 4059 (2016).
6. C. Wu, Y. Zou, T. Wu, M. Ban, V. Pecunia, Y. Han, Q. Liu, T. Song, S. Duhm, and B. Sun, "Improved performance and stability of all-inorganic perovskite light-emitting diodes by antisolvent vapor treatment," Adv. Funct. Mater. **27**, 1700338 (2017).
7. P. Xia, Y. Lu, Y. Li, W. Zhang, W. Shen, J. Qian, Y. Wu, W. Zhu, H. Yu, L. Liu, L. Deng, and S. Chen, "Solution-processed quasi-two-dimensional/nanoscrystals perovskite composite film enhances the efficiency and stability of perovskite light-emitting diodes," ACS Appl. Mater. Interfaces **12**, 39720 (2020).
8. L. Song, X. Guo, Y. Hu, Y. Lv, J. Lin, Z. Liu, Y. Fan, and X. Liu, "Efficient inorganic perovskite light-emitting diodes with polyethylene glycol passivated ultrathin $CsPbBr_3$ films," J. Phys. Chem. Lett. **8**, 4148 (2017).
9. Y. Meng, X. Wu, Z. Xiong, C. Lin, Z. Xiong, E. Blount, and P. Chen, "Electrode quenching control for highly efficient $CsPbBr_3$ perovskite light-emitting diodes via surface plasmon resonance and enhanced hole injection by Au nanoparticles," Nanotechnology **29**, 175203 (2018).
10. M. Y. Huang, L. Veeramuthu, C. C. Kuo, Y. C. Liao, D. H. Jiang, F. C. Liang, Z. L. Yan, R. Borsali, and C. C. Chueh, "Improving performance of Cs-based perovskite light-emitting diodes by dual additives consisting of polar polymer and n-type small molecule," Org. Electron. **67**, 294 (2019).
11. C. H. Gao, Y. Zhang, X. J. Ma, F. X. Yu, Y. L. Jia, Y. L. Lei, P. Chen, W. W. Sun, and Z. H. Xiong, "A method towards 100% internal quantum efficiency for all-inorganic cesium halide perovskite light-emitting diodes," Org. Electron. **58**, 88 (2018).
12. A. Subramanian, J. Akram, S. Hussain, J. Chen, K. Qasim, W. Zhang, and W. Lei, "Interfacial energy level alignment for high performance all-inorganic perovskite $CsPbBr_3$ quantum dots based inverted light emitting diodes," ACS Appl. Electron. Mater. **2**, 230 (2020).
13. Q. Khan, A. Subramanian, G. Yu, K. Maaz, D. Li, R. U. R. Sagar, K. Chen, W. Lei, B. Shabbir, and Y. Zhang, "Structure optimization of perovskite quantum dot light-emitting diodes," Nanoscale **11**, 5021 (2019).
14. X. J. Ma, Z. Q. Wang, Z. Y. Xiong, Y. Zhang, F. X. Yu, P. Chen, Z. H. Xiong, and C. H. Gao, "30-fold efficiency enhancement achieved in the perovskite light-emitting diodes," RSC Adv. **7**, 50571 (2017).
15. Y. Meng, M. Ahmadi, X. Wu, T. Xu, L. Xu, Z. Xiong, and P. Chen, "High performance and stable all-inorganic perovskite light emitting diodes by reducing luminescence quenching at PEDOT:PSS/perovskites interface," Org. Electron. **64**, 47 (2019).
16. Y. Zou, M. Ban, Y. Yang, S. Bai, C. Wu, Y. Han, T. Wu, Y. Tan, Q. Huang, X. Gao, T. Song, Q. Zhang, and B. Sun, "Boosting perovskite light-emitting diode performance via tailoring interfacial contact," ACS Appl. Mater. Interfaces **10**, 24320 (2018).
17. L. Tang, J. Qiu, Q. Wei, H. Gu, B. Du, H. Du, W. Hui, Y. Xia, Y. Chen, and W. Huang, "Enhanced performance of perovskite light-emitting diodes via diamine interface modification," ACS Appl. Mater. Interfaces **32**, 29132 (2019).
18. Q. Huang, J. Pan, Y. Zhang, J. Chen, Z. Tao, C. He, K. Zhou, Y. Tu, and W. Lei, "High-performance quantum dot light-emitting diodes with hybrid hole transport layer via doping engineering," Opt. Express **24**, 25955 (2016).
19. A. Subramanian, Z. Pan, Z. Zhang, I. Ahmad, J. Chen, M. Liu, S. Cheng, Y. Xu, J. Wu, W. Lei, Q. Khan, and Y. Zhang, "Interfacial energy level alignment for high performance all-inorganic perovskite $CsPbBr_3$ quantum dots based inverted light emitting diodes," ACS Appl. Mater. Interfaces **10**, 13236 (2018).
20. S. Hussain, A. Subramanian, S. Yan, G. Abbas, A. Shuja, W. Lei, and Q. Khan, "Engineering architecture of quantum dot-based light emitting diode for high device performance with double-sided emission fabricated by non-vacuum technique," ACS Appl. Electron. Mater. **8**, 2383 (2020).
21. W. J. E. Beek, M. M. Wienk, M. Kemerink, X. Yang, and R. A. J. Janssen, "Hybrid zinc oxide conjugated polymer bulk heterojunction solar cells," J. Phys. Chem. B **19**, 9505 (2005).
22. P. Jing, W. Ji, Q. Zeng, D. Li, S. Qu, J. Wang, and D. Zhang, "Vacuum-free transparent quantum dot light-emitting diodes with silver nanowire cathode," Sci. Rep. **5**, 12499 (2015).
23. L. Zhang, X. Yang, Q. Jiang, P. Wang, Z. Yin, X. Zhang, H. Tan, Y. M. Yang, M. Wei, B. R. Sutherland, E. H. Sargent, and J. You, "Ultra-bright and highly efficient inorganic based perovskite light-emitting diodes," Nat. Commun. **8**, 15640 (2017).